Determination of the dynamic deformability parameters in pastefill

Marco António dos Santos Candeias[1]
[1]Instituto Superior Técnico, Universidade de Lisboa, Portugal
marco.candeias@tecnico.ulisboa.pt

ABSTRACT

Herein the dynamical Young modulus of pastefill are studied, in laboratory and in situ, through the determination of seismic waves, in order to understand the scale effect in these mechanical parameters. In the field, a seismograph and two geophones were used to acquire seismic data in 6 benches with distinct curing time and for three depth levels, with equal cement percentage (5.5%). In the laboratory the seismic waves were assayed in samples (5.5% of cement), with piezoelectric sensors, and the static Young modulus were also obtained.

In the laboratory it was created a relation between the two deformability modulus (static and dynamical) with R2=0.6546. In the field the P wave velocities: increase with the increasing of the curing time; in the generality, there is an increase with the increasing of depth; a decrease with an increasing for the spacing between geophones. Using a multiple linear regression with R2=0.8597 it is evident that the curing time is the variable with highest influence regarding the behavior of the P waves velocities. This behavior repeats for the dynamical Young modulus in situ.

It is evident a relation between the decreasing of the scale of the study and the increasing of the dynamical Young modulus values, through a comparison between the two scales (laboratory and in situ), with a decrease of 33.43%, 39.30% e 63% for 1m, 12.5m e 23m, respectively.

To conclude it is notorious the influence of changing the scale of study in the dynamical Young modulus values.

Keywords

Young modulus, Scale effect, Pastefill, Non destructive testing, P-wave

1. INTRODUCTION

A mining exploitation will always create voids underground, which can condition the stability of the area involved. During this process the creation of enormous quantities of non-profitable material it is inevitable. These materials after chemical treatment are usually put in dams. In a perceptive way the extractive industry worldwide understood that they could use those materials as backfill. With this simple solution they contribute with an environmental sustainable policy, while at the same time, providing an increment of mining stability.

Pastefill is one of the several backfill types, resulting from the mixture of tailings, cement, water and from time to time additives. This mixture has to take account the technical and economical constraints. Pastefill will have to resist situations of a dynamic and static nature.

Then it is important to study the deformability of pastefill, and of course the associated parameters.

The Young modulus (E) represents the elasticity of a given material. There is a discrepancy in terms of the value of E for a rock and the backfill, regardless of the type of the fill used, where the rock is clearly superior (Brady & Brown, 2005). It is logical to study this parameter of pastefill, in order to better understand its behavior and consequently improve the exploitation methods. Not to mention the importance as far as potential rockburst is concerned (Hassani, Ouellet, & Servant, 2001).

If we want to access the dynamical information we can perform non destructive testing, highlighting the use of seismic. They are performed both in situ and laboratory (Ghafoori, Rastegarnia, & Lashkaripour, 2018).

Following this idea they can be used to infer about the difference of changing the scale, comparing both scales information. They could provide a full study of the scale effect on the Young modulus of pastefill.

Herein will be presented a study with the purpose of studying the influence of changing the scale in the values of Young modulus in pastefill. The analysis was carried both in the field and in the laboratory, results of which are compared.

2. CASE STUDY

2.1. .*Experimental Procedure in field*

During a seismic campaign in Neves Corvo Mine, data in 6 benches was acquired, with different curing time and distributed at 3 depth levels, only the cement percentage was constant (5.5%). This campaign was performed with 1 seismograph and 2 geophones, and only P waves were collected. The seismograph was an Instantel, model Minimate plus (series III) (Figure 1). The geophones were from two kinds, a standard and a low level (Figure 2) with a bandwidth of [2-250] Hz.

Figure 1 - Seismograph used in the seismic campaign

Figure 2 - Geophones used in the seismic campaign (on the left the standard geophone, and on the right the low level geophone)

The equipment was placed on top of a bench with pastefill exposed. The geophones were disposed within a known distance (spacing), and it was made a solicitation from a distance of 65cm from the first geophone. The solicitation was preserved during the entire campaign, using a weight of 807g released from a vertical height of 1m. In every single bench, 3 assessments were made according to the orientation of the Figure 3. For the X direction 2 assessments were made for a spacing of 1m and 12.5m, and another one with a spacing of 1m for the Y direction. In Figure 4 it is possible to observe the assays in 12.5m and 1m and the respective directions of acquisition. In every assessment it was perform 15 solicitations.

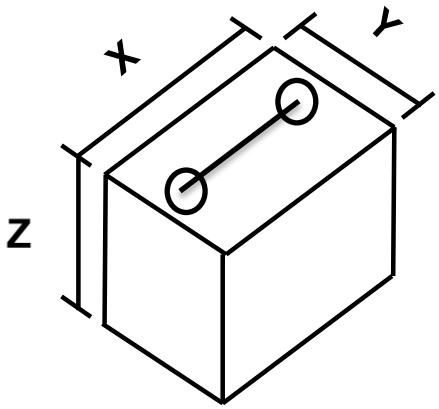

Figure 3 - The orientation of the geophones in the bench. X,Y and Z correspond respectively to length, width and height of the bench. It is demonstrated an example of the positioning of the geophones in the X direction.

The geophones are triorthogonal which means that they record data in 3 directions orthogonal to each other. For the calculations of the velocity of P-wave, the spacing is used as the distance and the arrival times as time. The latter is analyzed in seismograms, and taken as the difference between the wave arrivals at the 2 geophones. (**1**).

$$V_P = \frac{Spacing}{T_{geophone2} - T_{geophone1}} \qquad (\mathbf{1})$$

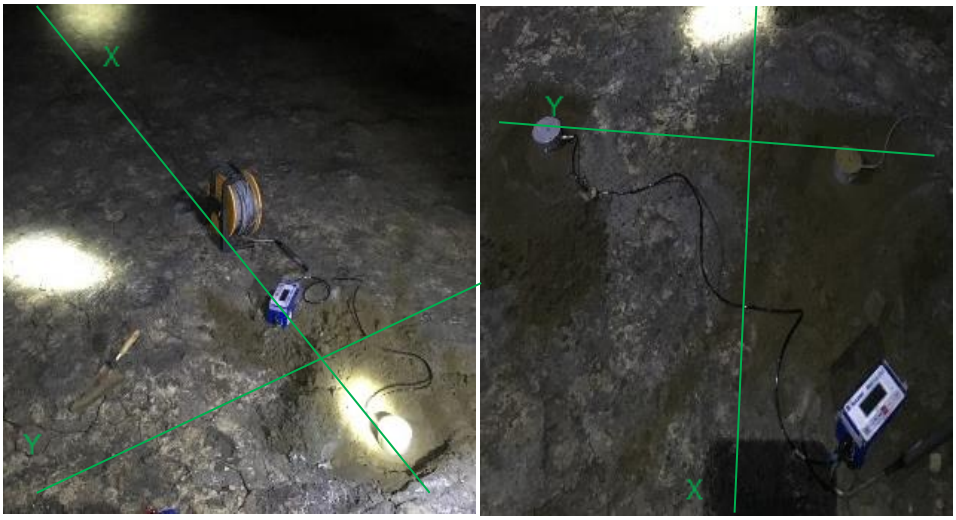

Figure 4 –Acquisition of the seismic data, on the left for a spacing of 12.5m and on the right for 1m, with the directions identified in the form of axis.

Besides all these information additionally there is an information concerning the trigger. The trigger is the minimum amplitude that initiates the recording. Since in every assessment 15 solicitations were performed, which means that the experiment was replicated under the same conditions, and the average values were considered. When performing these assays it is assumed that the direction of acquisition (the disposition of the geophones) is much bigger than the other two directions, in other words, a unidirectional propagation of the wave is assumed.

2.2. .*Experimental Procedure in laboratory*

The samples used in the laboratory assessments had the same cement percentage as the benches analyzed in field (5.5%), in a total of 10 samples, indexed as A1 to A5 and B1 to B5. The index A means they were collected in the industrial complex where the pastefill is produced, and the index B means they were collected *in situ*. The laboratory apparatus can be divided in two stages. The first one when it was perform the ultrasonic testing, in order to obtain the P and S wave velocities, according to the ultrasonic test procedure (ISRM, 2013), for studying the dynamical Young modulus. And a second stage with the purpose of studying the static Young modulus, by performing the uniaxial compressive strength assay according to the procedure (ISRM, 1979).

For measuring the arrival times for both waves 2 kinds of piezoelectric sensors were used, specialized in each wave. For P waves the sensors of model PXRw with a bandwidth between 80kHz and 400kHz were resorted, on the other hand for the S waves the sensors of model SWC37-0.5-SHEAR with a nominal frequency of 500kHz. Both sensors were connected to a signal generator BK PRECISION model 4011A with a bandwidth between 0.5Hz and 5MHz, and the frequency utilized was 50Hz. The visualization of the wave was done by an oscilloscope R&S®HMO1002 Series. Given that pastefill is a material that promotes phenomena of attenuation it was used a signal amplifier, with a capacity to amplify 200 times the signal. The former apparatus is shown in Figure 5.

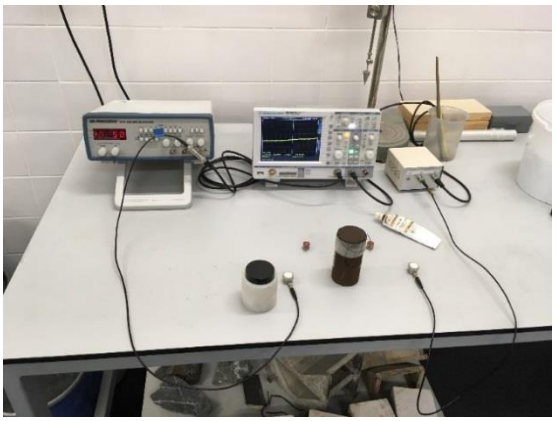

Figure 5- The laboratory apparatus for using the ultrasonic technique

For the uniaxial compressive strength test a lading cell FORM+TEST model Zwiefalter Straße 20 D-88499 Riedlinger, with a maximum load capacity of 1000kN, was used. The strain gauges were connected with a Data Tracker Model P3 Strain Indicator and Recorder. The static Young modulus was calculated by the tangent method.

3. RESULTS AND DISCUSSION

In this chapter, results from the laboratorial analysis are presented, followed by the field results. After this, a comparison of the results from both scales is presented.

3.1. . *Results from the Laboratory*

Only 8 of the initial samples were analyzed, because samples A1 and B3 were not in the conditions ascribed as (ISRM, 1979). For calculation the dynamical Young modulus the density value of 2409kg/m^3 was used, this value as given by the company. The results are shown in Table 1. The values of static Young modulus are lower compared with the dynamical Young modulus, which it was expected. The average value of static Young modulus is 0.430GPa and the dynamical is 0.775GPa, which means that the dynamical modulus is 1.8 times higher than the static modulus.

Table 1 - Results of the ultrasonic technique, with P and S velocities, static and dynamical Young modulus and Poisson ratio

Sample	Vp(m/s)	Average Vp (m/s)	Vs(m/s)	Average Vs (m/s	Es(GPa)	Ed(GPa)	v
A2	1188.64	1095.41	276.47	287.77	0.417	0.542	0.47
A3	1580.13		330.13		0.480	0.776	0.48
A4	758.99		290.83		0.392	0.576	0.41
A5	853.87		253.65		0.377	0.450	0.45
B1	1144.53	1218.97	336.08	369.81	0.422	0.791	0.45
B2	1273.88		329.87		0.423	0.768	0.46
B4	1308.62		425.61		0.480	1.258	0.44
B5	1148.85		387.69		0.450	1.040	0.44

It was perform an analysis between the two states in order to establish a relation, with a coefficient of determination of 0.6546 (Figure 6). It is evident a positive correlation between the two states.

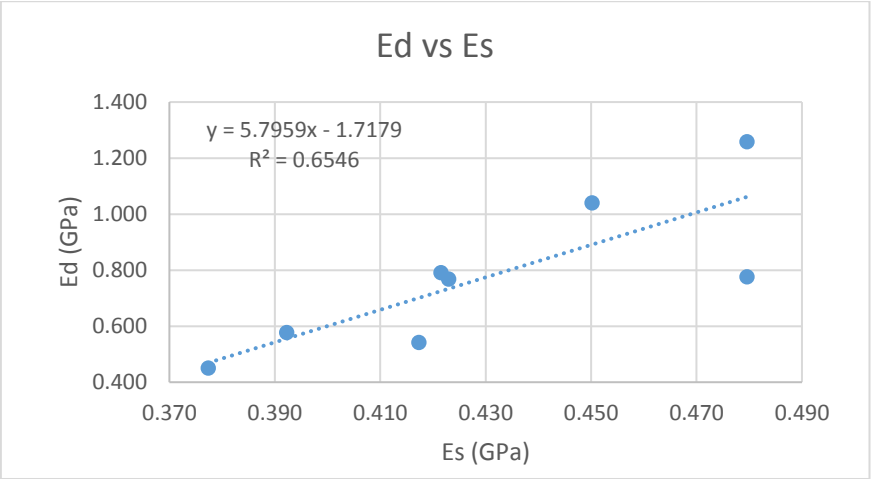

Figure 6 - Relation between the two Young modulus

3.2. . *Results from the field*

The directional velocities were not so different when compared to each other, admitting that these differences are included in the associated uncertainty, an isotropic medium can be assumed. .In order to know what value should be used, it was applied the trigger criteria. The Table 2 shows the results, using the trigger, of the velocities for the 6 benches for the assays performed. The values obtained are similar to those obtained by (Marta, 2018). The benches with the highest curing time (LS275B011,LS415B060,LS415B062) exhibit higher P-wave velocities(691m/s,566m/s,489m/s) respectively, considering the direction X as an example. Those evidence are in agreement with (Miranda, 2016), (Marta, 2018)). If the benches were grouped by depth (925m, 785m and 685m) it is evident that the highest depths lead to higher values of P-wave velocities. With an increasing of depth occurs an increment of the vertical stress, and according to (Miranda, 2016) increasing the vertical stresses leads to higher P-wave velocities. At a depth of 925m, it can be seen that the bench LS275B014 unexpectedly does not produce a very high value of velocities. Nevertheless, that particular bench has the lowest curing period and, as stated before, the curing time promotes higher velocities values.

Table 2 Results of velocities using trigger for the 6 benches, with different spacing, and information regarding the curing time and depth

L(m)	1	1	12.5	Starting curing time	Depth (m)
Direction	X	Y	X		
Bench	V (m/s)	V (m/s)	V (m/s)		
LS275B011	691	641	580	27/9/17	925
LS275B014	381	420	352	10/4/2018	925
LS415B060	566	542	550	2/9/2017	785
LS415B062	489	505	526	20/12/2017	785
LS515B112	373	373	363	20/3/2018	685
LS515B108	414	399	394	11/2/2018	685

In order to understand the contribution of the curing time in the P-wave velocities a linear regression was made for the 3 kinds of assays Figure 7, 8 and 9. It is evident that increasing the curing time promotes higher P-wave velocities, confirmed by the coefficient of determination.

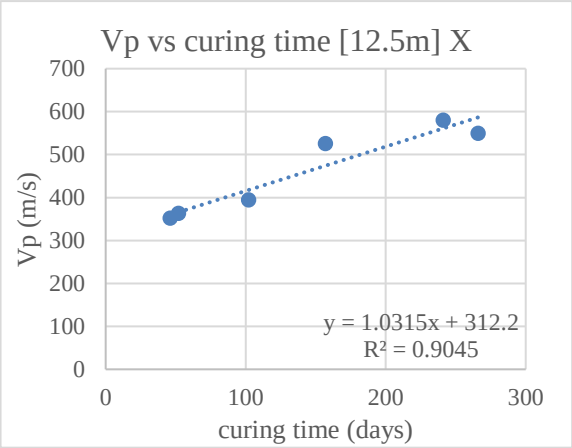

Figure 7 Scatterplot between curing time and P-wave velocity, for spacing 12.5m direction X.

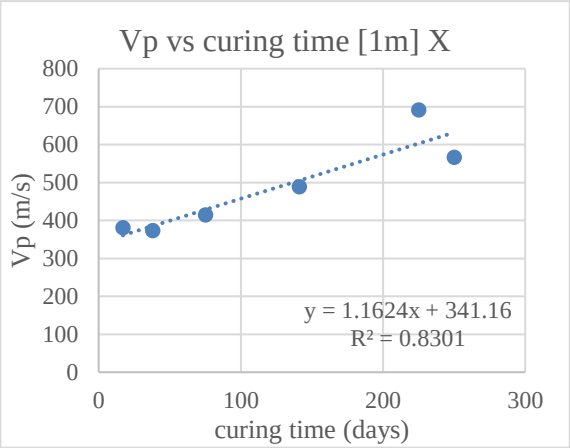

Figure 8 Scatterplot between curing time and P-wave velocity, for spacing 1 direction X.

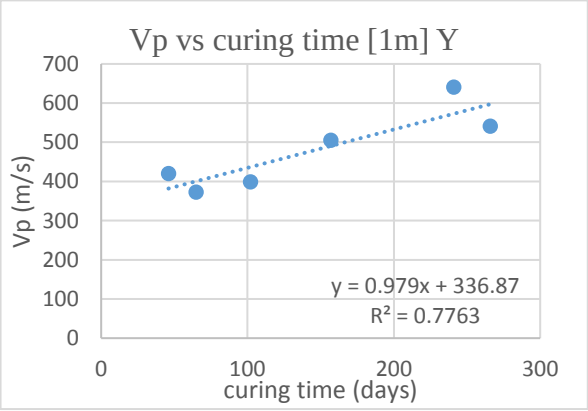

Figure 9-Scatterplot between curing time and P-wave velocity, for spacing 1m direction Y.

In regard to depth, Figure 10 demonstrates that higher depth produces higher values of P-wave velocities. Similarly, bench LS275B014 is from the depth level 925m but simultaneously has the lowest curing time. Besides that, the

influence of the variable depth is less noticeable for benches with similar curing times (levels 685m and 785m), and is more evident for benches with different curing times (level 925m).

In addition only one assessment for the spacing of 23m was performed, for the bench LS275B014. This approach was not made for all benches for technical reasons. For this spacing a value of 345m/s was obtained, for a curing period of 31 days. Figure 11 shows the tendency of decreasing the values of velocity while increasing the spacing. A reduction of 7.61% occurs, from 1m to 12.5m and 9.46% from 1 m to 23m.

Multiple linear regression were performed, using the 19 events. The independent variables were curing time and depth. The model is given by (**2**), and with a R^2= 0.8597. Where C stands for curing time, and P for depth.

$$Y = 154.3066 + 1.0149C + 0.2233P \qquad (2)$$

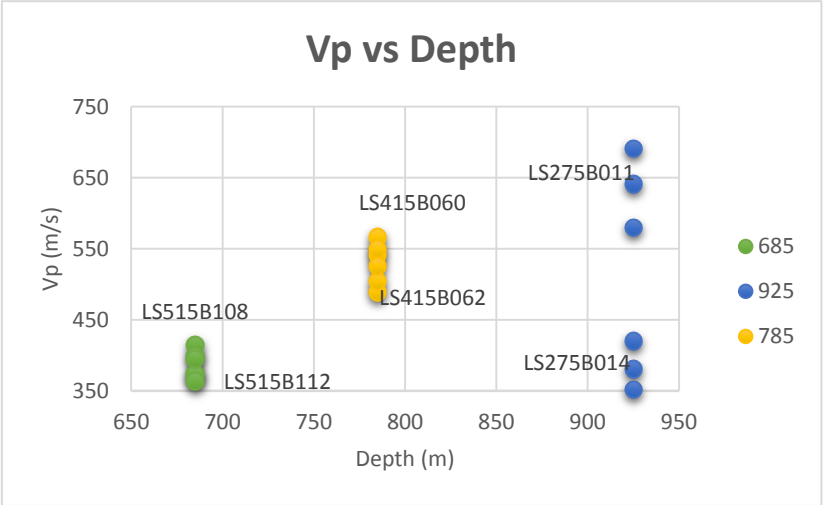

Figure 10- Relation between the P-wave velocities and the depth.

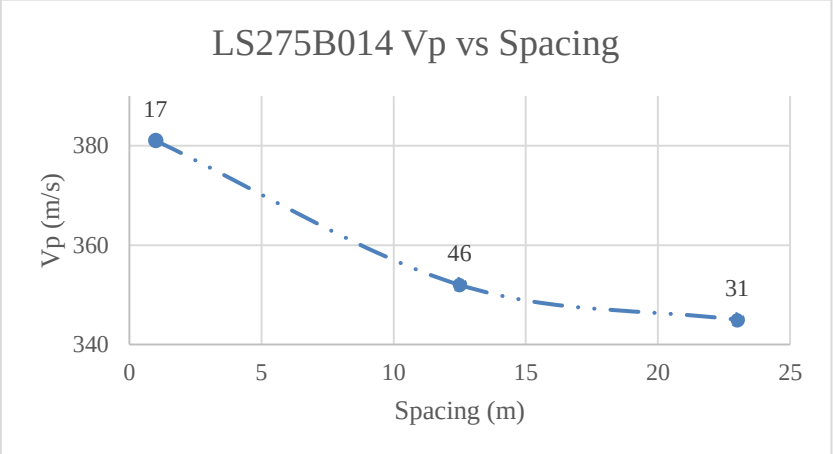

Figure 11 - Relation between P-wave velocities and spacing, with curing time identified.

Assuming unidirectional propagation the calculation of dynamical Young modulus is given by (Awang, Ahmad Rashidi, Yusof, & Mohammad, 2017) (**3**) using the same value for density as used for laboratory samples.

$$E_d = V_P^2 * \rho \qquad (3)$$

Table 3 gives all the information about all the assessments performed, including the dynamical Young modulus of the benches. The conditioning verified for the P-waves velocities are the same as those regarding the dynamical

Young modulus. Higher curing time promotes higher values of the modulus. A similar relation was observed for the depth variable, in which higher depth promotes higher values of the modulus. The Figure 12 shows the influence of increasing the spacing, which in returns gives a decrease of the values of the dynamical Young modulus. From 1m to 12.5m there is a reduction of 8.81%, and from 1m to 23m a reduction of 44.42% for the dynamical Young modulus.

Table 3 – information regarding all the assessments performed, highlighting the dynamical Young modulus

Bench	V (m/s)	Curing time (days)	Depth (m)	Direction	Spacing (m)	Ed (GPa)
LS515B108	414	75	685	X	1	0.414
LS515B112	373	38	685	X	1	0.335
LS275B014	381	17	925	X	1	0.349
LS275B011	691	225	925	X	1	1.151
LS415B060	566	250	785	X	1	0.772
LS415B062	489	141	785	X	1	0.575
LS515B108	399	102	685	Y	1	0.383
LS515B112	373	65	685	Y	1	0.335
LS275B014	420	46	925	Y	1	0.425
LS275B011	641	241	925	Y	1	0.990
LS415B060	542	266	785	Y	1	0.706
LS415B062	505	157	785	Y	1	0.614
LS515B108	394	102	685	X	12.5	0.375
LS515B112	363	52	685	X	12.5	0.318
LS275B014	352	46	925	X	12.5	0.298
LS275B011	580	241	925	X	12.5	0.810
LS415B060	550	266	785	X	12.5	0.728
LS415B062	526	157	785	X	12.5	0.666
LS275B014	345	31	925	X	23	0.287

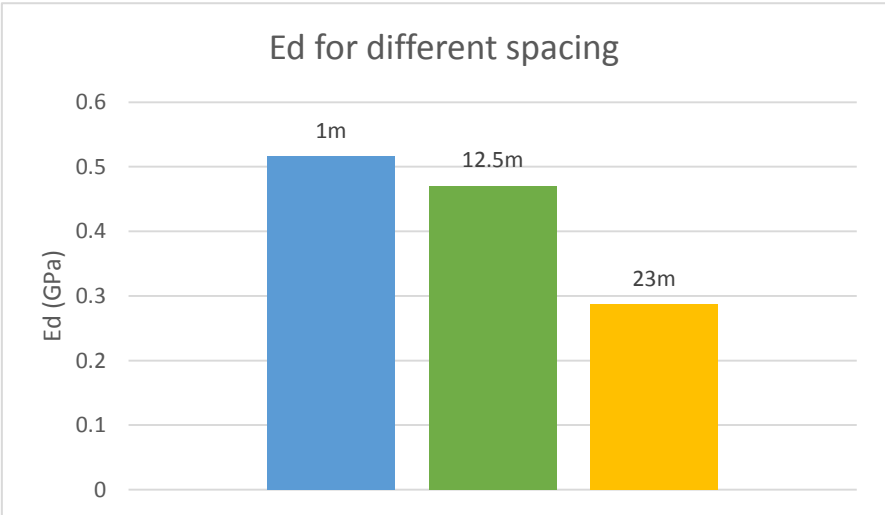

Figure 12- Dynamical Young modulus for the spacing of 1m, 12.5 and 23m

3.3. .*Comparison in both scales*

The two scales are now compared with averaged values. The average value of the dynamical Young modulus for the samples is 0.775GPa. Figure 13 shows the values for all the scales studied. A huge difference in values is evident for all scales. The dynamical Young modulus decreased by 33.43% when changing the laboratory scale to the field scale of 1m spacing, 39.30% for the 12.5m and 63% for 23m. It is notorious the influence of the scale on the analysis in what concerns the dynamic Young modulus.

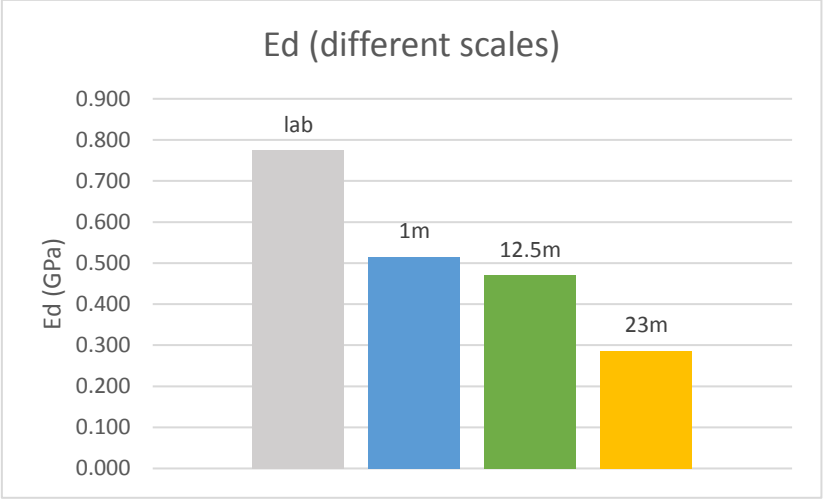

Figure 13 - Values of the dynamical Young modulus for the different scales analyzed in this study

4. CONCLUSION

The directional velocities do not diverge between themselves in an expressive form, from which we can assume a state of isotropy. Only one velocity was used, which is originated by the trigger criteria.

The results show that curing time and depth variables have an influence over the velocities of propagation. Curing time presents a coefficient of determination (R^2): of 0.9045 for a spacing of geophones of 12.5m in the direction of acquisition X; of 0.8031 for a spacing between geophones of 1m in the direction of acquisition X; of 0.7763 for a spacing between geophones of 1m in the direction of acquisition Y.

An increase in depth led to higher values in velocity, with the exception of a bench (LS275B014) which presented the lowest curing time of the study. The influence of the variable depth is less noticeable for benches with similar curing times (levels 685m and 785m), and is more evident for benches with different curing times (level 925m).

With an increase in spacing from 1m to 12.5m, a decrease in velocity of 7.61% was verified, while the decrease registered is of 9.46% for a spacing between 1m to 23m.

Multiple linear regression was performed with a determination coefficient R^2=0.8597.

In the case of the laboratorial assays, the values of the dynamical deformability modulus are around 1.8 times higher than the static deformability modulus. A correlation between the values of the static elasticity modulus and the dynamic elasticity modulus was made, from which a coefficient of determination R^2=0.6546 was obtained. In the field it is evident, that the variables that condition P wave velocity have the same effect for dynamical Young modulus in situ. It is noted that Curing time has an enormous influence on dynamic Young modulus. Hence, the values of the modulus increase with depth, decrease with the increase in spacing between geophones, as verified with P-wave velocity.

Comparing values obtained in the field with the ones obtained in the laboratory, a decrease in the value of the deformability modulus with the increase in dimension is notorious. At a laboratorial scale, a 0.775GPa average value was obtained. In the field, values were lower by a rate of 33.43% for a spacing of geophones of 1m, 39.30% for a spacing of 12.5m and 63% for a spacing of 23m.

We can conclude that the scale study is determinant for the deformability analysis.

References

Awang, H., Ahmad Rashidi, N. R., Yusof, M., & Mohammad, K. (2017). Correlation Between P-wave Velocity and Strength Index for Shale to Predict Uniaxial Compressive Strength Value. *MATEC Web of Conferences . 103, 07017.* International Symposium on Civil and Environmental Engineering 2016.

Brady, B., & Brown, E. (2005). *Rock Mechanics for underground mining* (3rd ed.). Springer Science + Business Media, Inc.

Ghafoori, M., Rastegarnia, A., & Lashkaripour, G. R. (2018). Estimation of static parameters based on dynamical and physical properties in limestone rocks. *Journal of African Earth Sciences, 137*, pp. 22-31.

Hassani, F., Ouellet, J., & Servant, S. (2001). In Situ Measurements in a Paste Backfill: Backfill and Rock Mass Response in the Context of Rockburst . *Proceedings of the 17th International Mining Congress and Exhibition of Turkey*, (pp. 165-175).

ISRM. (1979). Suggested methods for determining the uniaxial compressive strength and deformability of rock materials. *International Journal of Rock Mechanics and Mining Sciences & Geomechanics Abstracts, 16*(2), pp. 137-140.

ISRM. (2013). Upgraded ISRM Suggested Method for Determining Sound Velocity by Ultrasonic Pulse Transmission Technique. (R. Ulusay, Ed.) *The ISRM Suggested Methods for Rock Characterization, Testing and Monitoring: 2007-2014*, pp. 95–99.

Marta, A. (2018). *Relação entre a velocidade das ondas P e das ondas S e a deformação no paste fill.* Master's Thesis in Mining and Geological Engineering, Instituto Superior Técnico, Lisbon.

Miranda, M. (2016). *Contribuição para a determinação do estado de tensão no enchimento mineiro através da medição das ondas sísmicas.* Master's Thesis in Mining and Geological Engineering, Instituto Superior Técnico, Lisbon.